Report

Current Biology

Auxin Acts through MONOPTEROS to Regulate Plant Cell Polarity and Pattern Phyllotaxis

Graphical Abstract

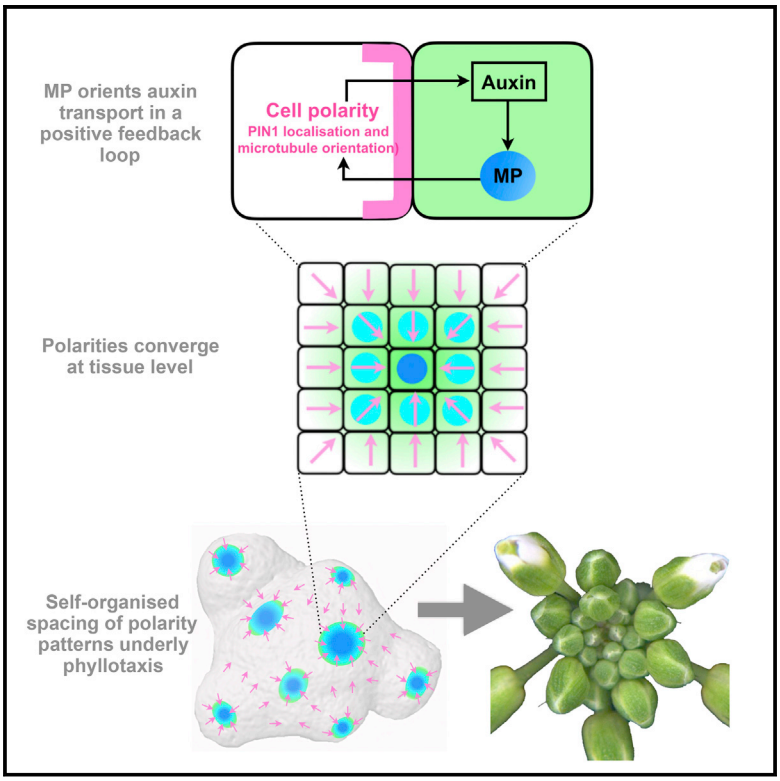

Authors

Neha Bhatia, Behruz Bozorg, André Larsson, Carolyn Ohno, Henrik Jönsson, Marcus G. Heisler

Correspondence

heisler@embl.de

In Brief

Organ positioning in plants depends on polar transport of the hormone auxin to organ initiation sites. Bhatia et al. reveal that the auxin response factor MONOPTEROS orients the polarity of the auxin efflux carrier PIN1 non-cell autonomously, thereby facilitating a positive feedback loop that results in periodic organ formation.

Highlights

- Auxin-regulated MP expression and activity predict PIN1 polarity changes at the SAM
- Localized MP activity is necessary to mediate periodic organ formation
- MP orients PIN1 polarity non-cell autonomously to promote local auxin accumulation
- Sub-epidermal MP activity is required to stabilize auxin distribution patterns

Bhatia et al., 2016, Current Biology *26*, 1–7
December 5, 2016
http://dx.doi.org/10.1016/j.cub.2016.09.044

CellPress

Please cite this article in press as: Bhatia et al., Auxin Acts through MONOPTEROS to Regulate Plant Cell Polarity and Pattern Phyllotaxis, Current Biology (2016), http://dx.doi.org/10.1016/j.cub.2016.09.044

Current Biology
Report

Auxin Acts through MONOPTEROS to Regulate Plant Cell Polarity and Pattern Phyllotaxis

Neha Bhatia,[1] Behruz Bozorg,[2] André Larsson,[2] Carolyn Ohno,[1] Henrik Jönsson,[2,3] and Marcus G. Heisler[1,4,5,*]
[1]European Molecular Biology Laboratory, Meyerhofstrasse 1, 69117 Heidelberg, Germany
[2]Computational Biology and Biological Physics Group, Department of Astronomy and Theoretical Physics, Lund University, Sölvegatan 14A, SE-223 62 Lund, Sweden
[3]Sainsbury Laboratory and Department of Applied Mathematics and Theoretical Physics, University of Cambridge, Cambridge CB2 1TN, UK
[4]Biological Sciences, The University of Sydney, Sydney, NSW 2006, Australia
[5]Lead Contact
*Correspondence: heisler@embl.de
http://dx.doi.org/10.1016/j.cub.2016.09.044

SUMMARY

The periodic formation of plant organs such as leaves and flowers gives rise to intricate patterns that have fascinated biologists and mathematicians alike for hundreds of years [1]. The plant hormone auxin plays a central role in establishing these patterns by promoting organ formation at sites where it accumulates due to its polar, cell-to-cell transport [2–6]. Although experimental evidence as well as modeling suggest that feedback from auxin to its transport direction may help specify phyllotactic patterns [7–12], the nature of this feedback remains unclear [13]. Here we reveal that polarization of the auxin efflux carrier PIN-FORMED 1 (PIN1) is regulated by the auxin response transcription factor MONOPTEROS (MP) [14]. We find that in the shoot, cell polarity patterns follow MP expression, which in turn follows auxin distribution patterns. By perturbing MP activity both globally and locally, we show that localized MP activity is necessary for the generation of polarity convergence patterns and that localized MP expression is sufficient to instruct PIN1 polarity directions non-cell autonomously, toward MP-expressing cells. By expressing MP in the epidermis of *mp* mutants, we further show that although MP activity in a single-cell layer is sufficient to promote polarity convergence patterns, MP in sub-epidermal tissues helps anchor these polarity patterns to the underlying cells. Overall, our findings reveal a patterning module in plants that determines organ position by orienting transport of the hormone auxin toward cells with high levels of MP-mediated auxin signaling. We propose that this feedback process acts broadly to generate periodic plant architectures.

RESULTS AND DISCUSSION

PIN1 Polarity Patterns Follow Auxin-Regulated MP Expression

Because MONOPTEROS (MP) transduces a transcriptional response from auxin required for flower formation [14, 15], we reasoned that feedback from auxin to its transport direction might occur via MP. To investigate this possibility, we first examined the expression pattern of a rescuing MP translational fusion to yellow fluorescent protein for energy transfer (YPet) (*pMP::MP-YPet*) in the shoot apical meristem (SAM) in comparison to PIN1 fused to CFP (PIN1-CFP), and found striking correlations in their localization patterns (Figures 1A–1C). However, we found that MP marked position i4 (incipient primordium 4) prior to a PIN1 convergence appearing at this site (n = 7 out of 7) (Figure 1D; Movie S1). And, although MP and PIN1 showed a strong correlation at the i3 stage (Figure 1E), a decrease in MP expression could be detected surrounding i1 prior to the characteristic reversal of PIN1 polarity toward adjacent regions [6] (Figures 1F and 1G). To compare MP expression to auxin distribution patterns, we also examined expression of the ratiometric auxin marker R2D2 [16] and found its expression pattern to appear almost identical to that of MP (Figures S1A–S1J). To test whether MP expression is patterned by auxin in the shoot, as found for other tissues [17, 18], we treated meristems expressing both MP-YPet and R2D2 with auxin or N-1-napthylphthalamic acid (NPA) and found a similar response (Figures S1K–S1R), with higher levels of MP-YPet transcripts being detected upon auxin treatment (Figure S1S), confirming that auxin levels tightly regulate MP expression. Overall, these data are consistent with auxin and MP acting upstream of PIN1 polarity changes during early organ formation.

Localized MP Activity Is Required for Localized Organ Initiation

To test whether localized MP expression is required for PIN1 polarity convergence patterns, we examined plants in which *MP* cDNA was induced under the control of the ubiquitin-10 promoter (*pUBQ10*) using dexamethasone (DEX) but found no obvious associated phenotype. However, examination of *pUBQ10>>MPc-YPet* expression within these plants revealed that MP was still expressed dynamically and remained correlated with PIN1 polarities, similar to the wild-type (Figure S2A). To test whether MP expression in these plants was still responsive to auxin, we monitored *pUBQ10>>MPc-YPet* expression in response to 1-Napthaleneacetic acid (NAA) application and observed an increase and broadening of expression (Figures S2B and S2C). To test whether the *pUBQ10* promoter was auxin responsive, we checked the meristems of control plants expressing *pUBQ10::H2B-2XGFP* and found that GFP was expressed more uniformly and did not get upregulated upon auxin addition

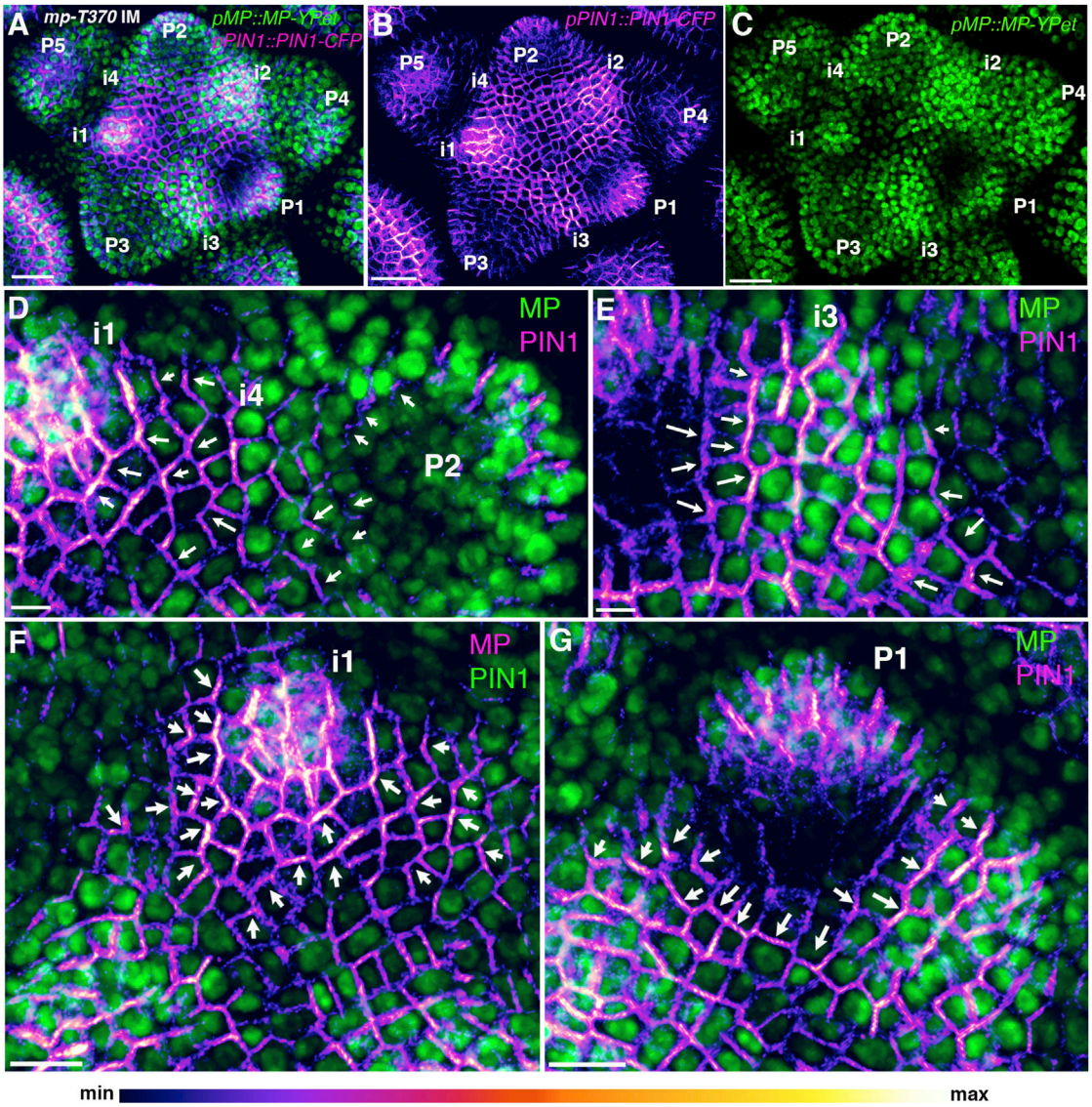

Figure 1. *MP* Expression Patterns Predict PIN1 Polarity Changes

(A) *pMP::MP-YPet* (green) and *pPIN1::PIN1-CFP* (magenta) expression and localization in the *mp-T370* inflorescence meristem (IM).

(B) Meristem in (A) showing *pPIN1::PIN1-CFP* alone.

(C) Meristem in (A) showing *pMP::MP-YPet* expression alone.

(D) Magnified view of i4 before PIN1 polarity convergence.

(E) Magnified view of i3 after PIN1 convergence.

(F) Magnified view of i1. Note the low MP expression surrounding i1 prior to PIN1 polarity reversal.

(G) Magnified view of P1 showing reduced MP expression surrounding the primordium and PIN1 polarity oriented away from low-MP-expressing cells.

The arrows indicate the estimated PIN1 polarity direction within the cells. Primordium (P) and incipient primordium (i) stages are numbered i4–P5. Scale bars, 30 μm (A–C), 5 μm (D and E), and 10 μm (F and G). See also Figure S1 and Movie S1.

(Figures S2D and S2E). This indicates that *cis*-elements within the coding region may contribute to the regulation of MP expression by auxin. To further disrupt MP expression, we engineered silent mutations in several putative auxin-response elements within the MP-coding region (Figure S2F) and induced this modified cDNA using the *UBQ10* promoter (*pUBQ10>>YPet-MPc mut*) in wild-type plants. Even though this modified cDNA was expressed more uniformly and did not respond to exogenous auxin application (Figures S2G–S2I), no phenotype in terms of organ positioning was observed in wild-type seedlings and inflorescences (Figures S2J–S2M). We reasoned that endogenous MP expression may still facilitate the formation of instructive MP gradients in the presence of uniform transgene expression, and thus transformed this construct into *mp* mutants. Although transformed *mp* mutant seedlings again showed no obvious phenotype (Figures S2N–S2Q), in *mp* mutant inflorescence meristems uniform expression of *YPet-MPc mut* resulted in the ectopic growth and lateral fusion of bract-like organs subtending floral meristems (Figures S2R and

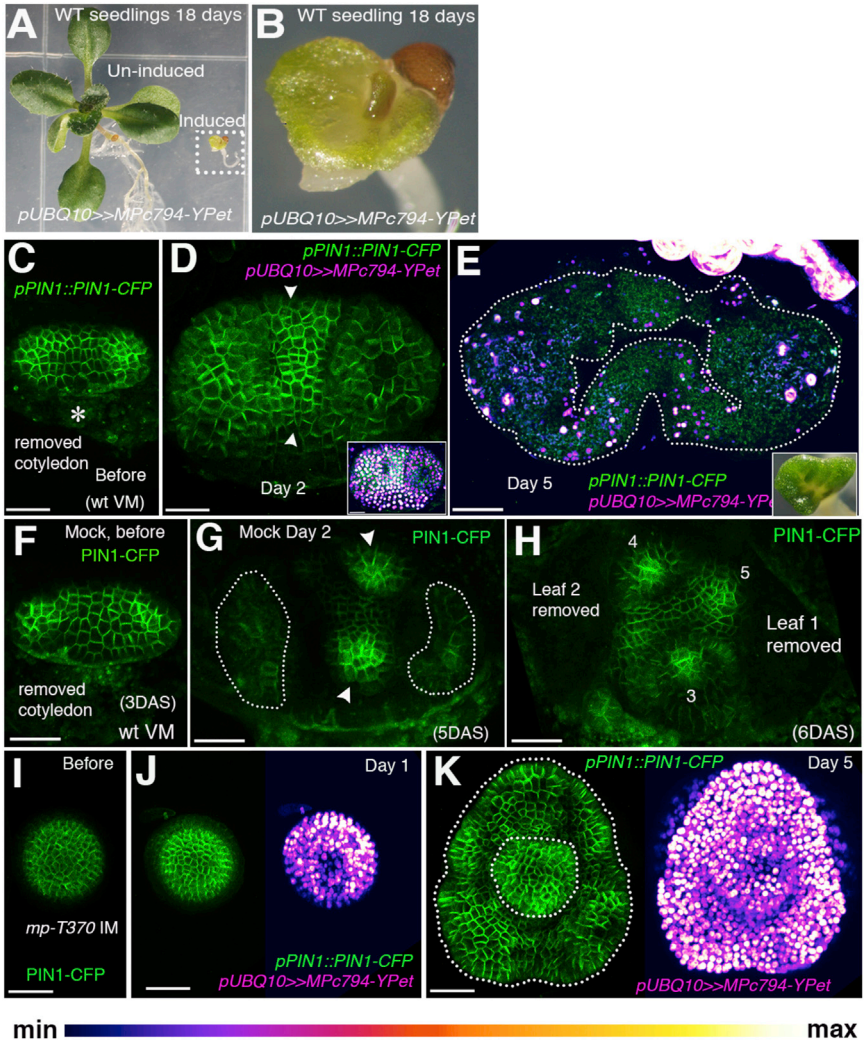

Figure 2. Localized Organogenesis Requires Localized MP Activity

(A) Wild-type seedling 18 days after induction of *pUBQ10>>MPc794-YPet* (dotted rectangle) in comparison to an un-induced plant.

(B) Magnified view of an induced plant from (A). Note the fusion of the first two leaves.

(C–H) *pPIN1::PIN1-CFP* expression and polarity (green) after induction of *pUBQ10>>MPc794-YPet* (C–E) compared to mock-treated seedlings (F–H) before treatment (C and F), 2 days later (D and G), and 5 days later (E and H). Note the absence of PIN1 convergences (arrowheads) in (D) compared to (G). Five days after *MPc794-YPet* induction a ring of organ tissue has developed (outlined by dotted line in E) that is absent in mock-treated control (H). The inset in (D) shows *MPc794-YPet* expression (magenta). The inset in (E) shows the phenotype after 11 days of *MPc794-YPet* induction (66%, n = 21).

(I–K) *pPIN1::PIN1-CFP* expression and polarity (green) before (I) and after induction of *pUBQ10>>MPc794-YPet* (magenta) (J and K) in *mp* IM. Note the ring-shaped organ present 5 days after *MPc794-YPet* induction (K).

The asterisk in (C) marks the removed cotyledon. Scale bars, 30 μm (C, D, and F–K) and 50 μm (E).

S2S). Thus, modulation of MP expression is essential to suppress bract growth and fusion, but not for specifying periodic positions.

To further investigate the role of MP activity in regulating organ formation and cell polarity, we truncated MP-YPet to create a constitutively active form of MP, in which domains III and IV are deleted [19]. Although prolonged induction of this form of MP in both wild-type and *mp* mutants led to transgene silencing, by imaging plants soon after induction we observed an absence of distinct PIN1 polarity convergence patterns and the initiation of non-localized growth at the meristem periphery (Figures 2A–2E and 2I–2K). The development of subsequent organs was seldom observed. Mock-treated wild-type control plants showed normal phyllotactic patterning (Figures 2F–2H). These data show that localized MP activity is required for localized PIN1 polarity convergence patterns and organogenesis, indicating that MP activity plays an instructive rather than permissive role in regulating organ position.

MP Orients PIN1 Localization Non-Cell Autonomously

To test whether MP feeds back on its own patterns of activation by directing auxin transport, we utilized Cre-Lox-mediated recombination to generate clones of cells expressing a functional *MP* gene fused to either *VENUS* or *YPet* under the *UBQ10* promoter in two loss-of-function *mp* mutant backgrounds (*mp-T370* and *mp-B4149*). PIN1 polarity was monitored using functional fusions to both GFP and CFP. Eight days after induction of Cre activity in the central zone of *mp* mutant meristems using DEX-inducible Cre-GR (glucocorticoid receptor) under the control of the *CLAVATA3* promoter [20, 21], we observed organ-like outgrowths associated with MP clones that were not there previously (Figures 3A and 3B). Time-lapse imaging revealed that clones expressing MP first appeared 3 days after DEX treatment. Strikingly, localization of PIN1 started to shift in neighboring cells toward these clones as they were displaced into the peripheral zone (Figures 3C–3M and S3H–S3J; Movie S2). We also noted a gradual increase in MP and PIN1 expression level within the clones over time, with PIN1 expression decreasing in adjacent regions farther away (Figures 3E–3H, 3J–3M, and S3B–S3G), indicating the local accumulation of auxin within the clones and the depletion nearby. By 6 days, the clones had formed outgrowths with PIN1 polarity convergence points at their distal tip (Figures 3H and S3E). In addition to observing polarity responses in epidermal cells adjacent to the clones, we also observed PIN1 polarity responses in cells underlying these clones (Figure 3N). Furthermore, we observed several examples in which MP clones were located in the L2 (layer 2) and, in these cases, we also observed PIN1 polarity convergence patterns in L2 and the overlying epidermis (Figures 3O–3Q). These results demonstrate that local MP expression is sufficient to polarize cells in a non-cell-autonomous manner in multiple cell layers,

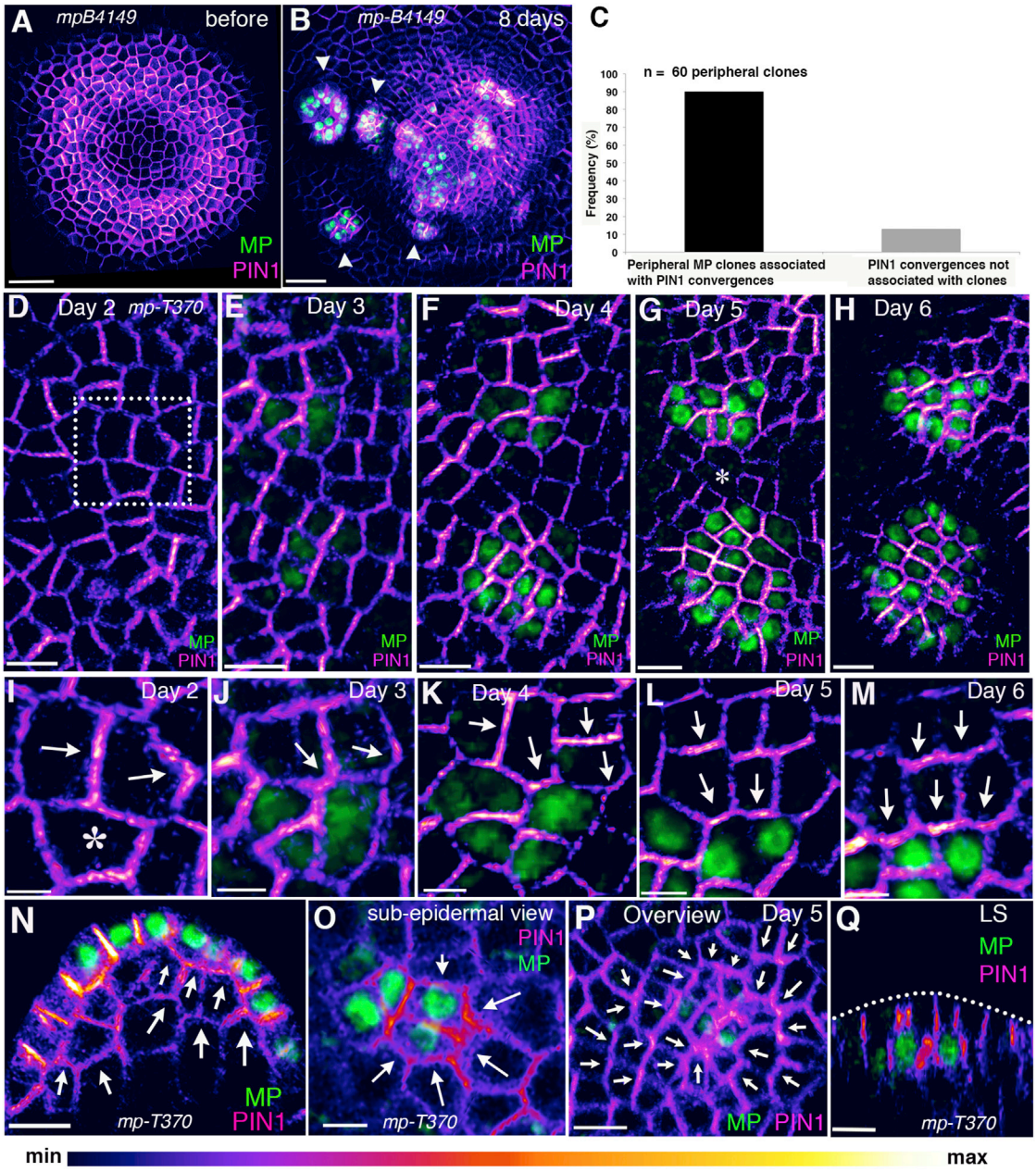

Figure 3. MP Polarizes Cells Non-Cell Autonomously

(A and B) Confocal projection showing the *mp-B4149* apex expressing *pPIN1::PIN1-GFP* (magenta) before (A) and 8 days after induction of MP-YPet clones (B) (green); arrowheads indicate initiating organs coinciding with MP expression.

(C) Frequency of peripheral MP clones associated with PIN1 convergence patterns (n = 60 peripheral clones of MP).

(D–M) Time series showing epidermal MP-VENUS clones in *mp-T370* and associated changes in PIN1-CFP localization.

(D–H) Overview showing two independent clones. Note the gradual increase in expression of both MP and PIN1 within the clones indicating an increase in local auxin levels compared to neighboring regions (asterisk in G).

(I–M) Magnified view of the dotted rectangle in (D). The asterisk in (I) marks the cell before MP-VENUS induction, corresponding to the future clone.

(N) Longitudinal optical section showing a sub-epidermal polarity response to the epidermal clone.

(O) Cross-section showing lateral PIN1 polarity toward the MP clone in the sub-epidermal layer.

(P) PIN1-CFP convergence in the epidermal cell layer in response to a sub-epidermal MP clone.

(Q) Longitudinal reconstructed section of (P) showing a sub-epidermal MP-VENUS clone.

The arrows indicate the estimated PIN polarity direction within the cells. Scale bars, 30 μm (A and B), 10 μm (D–H and N–Q), 4 μm (I), and 5 μm (J–M). See also Figures S3 and S4 and Movies S2 and S3.

and imply that auxin-induced transcriptional targets positively feed back on their own expression by influencing auxin transport. Because MP triggers gene expression in response to signaling by transport inhibitor response (TIR)1, which is localized intracellularly [22–24], this result also strongly supports previous models for phyllotaxis that assume that high levels of intracellular auxin act to polarize PIN1 in neighboring cells [7, 8, 10].

Because several previous studies have suggested a role for mechanical stresses in orienting cell polarity [10, 25, 26], and local MP expression most likely alters such stresses by promoting organ growth, we investigated whether a previously proposed model linking intracellular auxin to wall stresses and PIN1 localization [10] could account for the polarity patterns we observed in response to local MP expression. This model assumes that intracellular auxin promotes the expression of cell wall enzymes that loosen cell walls and that cells target their PIN1 protein toward membranes adjacent to highly stressed walls. Due to the common tensile load borne by attached, adjacent cell walls, the loosening of one cell wall triggered by auxin is assumed to increase the tensile stress on the adjacent cell wall, thereby promoting polarization of PIN1 in the adjacent cell toward the neighboring cell with high levels of intracellular auxin [10]. Using a finite element mechanical model of meristem tissue (see the Supplemental Experimental Procedures), we assumed that auxin-induced MP activity triggers cell wall loosening and simulated this loosening in small patches of cells in different cell layers to determine the predicted polarities of surrounding cells. We found this model could recapitulate polarity responses to epidermal MP clones (Figures S4A and S4B) and sub-epidermal polarity response to sub-epidermal clones (Figure S4C). In contrast, the predicted epidermal polarities to sub-epidermal clones did not match observations (Figure S4D). However, adding low levels of loosening in the overlying epidermal cells could restore a match to the simulations (Figure S4E), suggesting that residual auxin response may exist in non-MP-expressing cells. We tested this prediction by applying auxin to *mp* mutant meristems and observed a delayed PIN1 expression and limited growth response that could be inhibited by the TIR1 inhibitor auxinole (Figures S4F–S4M). These results confirm that residual TIR1-dependent auxin activity remains in *mp* mutants and that if this is taken into account, our results are consistent with a mechanical stress feedback model. Simultaneous observation of microtubule orientations together with PIN1 in response to MP clones also revealed correlated responses consistent with mechanical model predictions [26] (Figures S4N and S4O; Movie S3).

Sub-epidermal MP Activity Stabilizes Auxin Distribution Patterns to Underlying Cells

Because MP clones are sufficient to reorient PIN1 polarities toward the clones in multiple cell layers, we decided to express MP only in the epidermis to test whether epidermal expression of MP per se is sufficient to generate periodic patterns. In wild-type plants expressing MP-YPet under the control of the *MERISTEM LAYER 1* (*ML1*) promoter, we observed MP-YPet expression to be restricted to the epidermis but patterned in a similar way to the wild-type, and it remained auxin responsive (Figures 4A and 4B). To verify that the *pML1* promoter was not auxin responsive, we checked the meristems of control plants expressing *pML1::2X-CFP-N7* and found that CFP was uniformly expressed and did not show an increase in expression upon auxin application (Figures 4C and 4D). In contrast, many transgenic generation 2 (T2) *mp* mutant plants expressing MP in the epidermis developed fused cotyledons (23%, n = 13; 50%, n = 10) and leaves (Figures 4E and 4F). Although some of these plants failed to develop beyond the seedling stage, less severely affected plants (33%; n = 26, 20) underwent the transition to flowering. Of 13 such plants, 10 exhibited two elongated PIN1 polarity convergence and MP expression foci positioned on opposite sides of the SAM, with two distinct spirals of organ tissue forming continuous bands leading down the stem (Figures 4G–4I). Other configurations included a single spiral, a whorled pattern, and a whorled/spiral intermediate. Time-lapse imaging of plants exhibiting the spiral pattern revealed that in contrast to the wild-type situation, the expression patterns of both PIN1 and MP tended to shift laterally, along with convergent patterns of PIN1 polarity (Figures 4J and 4K). Although the initiation of organ growth correlated with the onset of high MP expression, this growth continued after the local maximum of MP and PIN1 expression subsequently shifted, thereby creating a continuous spiral of organ tissue. Longitudinal reconstructions of optical sections confirmed that whereas both PIN1-CFP and MP-YPet were upregulated in epidermal tissues, both markers were largely absent in cells below (Figures 4L and 4M). Notably, no evidence of pro-vascular tissue marked by PIN1 was detected (Figure 4M). Because vascular tissues have been associated with auxin depletion [27], we tested whether auxin-triggered auxin depletion could act to stabilize auxin distribution patterns generated by a previously proposed feedback model for auxin transport consistent with our findings [28] (see the Supplemental Experimental Procedures). We found that without negative feedback on auxin concentrations, the auxin maxima generated by this model could easily shift with respect to the underlying cells due to saturation of the transport system, leading to diffusion or "leakage" of auxin laterally [28] (Movie S4). However, by depleting auxin levels in an auxin-dependent manner, the locations of auxin maxima can be stabilized (Movie S4). These findings demonstrate that although MP is sufficient in a single-cell layer to mediate the formation of separated auxin maxima (corresponding to the two foci of MP and PIN1 expression observed at the apex), consistent with previous studies [29], additional MP-regulated processes in sub-epidermal tissues such as auxin depletion must exist that prevent movement of spacing patterns with respect to the underlying cells.

Although tissue-level cues orienting cell polarity in animals appear to be patterned independent of their downstream polarity targets, our data indicate that plants utilize cell polarity to propagate a mobile signal that acts within cells to orient the polarity of neighboring cells such that the signal accumulates locally. Having established MP as a central player in this feedback system, a future focus on MP target genes should ultimately lead to a molecular understanding of the signaling processes involved and how these processes are modulated in different plant species and tissue contexts to generate morphological diversity.

SUPPLEMENTAL INFORMATION

Supplemental Information includes Supplemental Experimental Procedures, four figures, two tables, and four movies and can be found with this article online at http://dx.doi.org/10.1016/j.cub.2016.09.044.

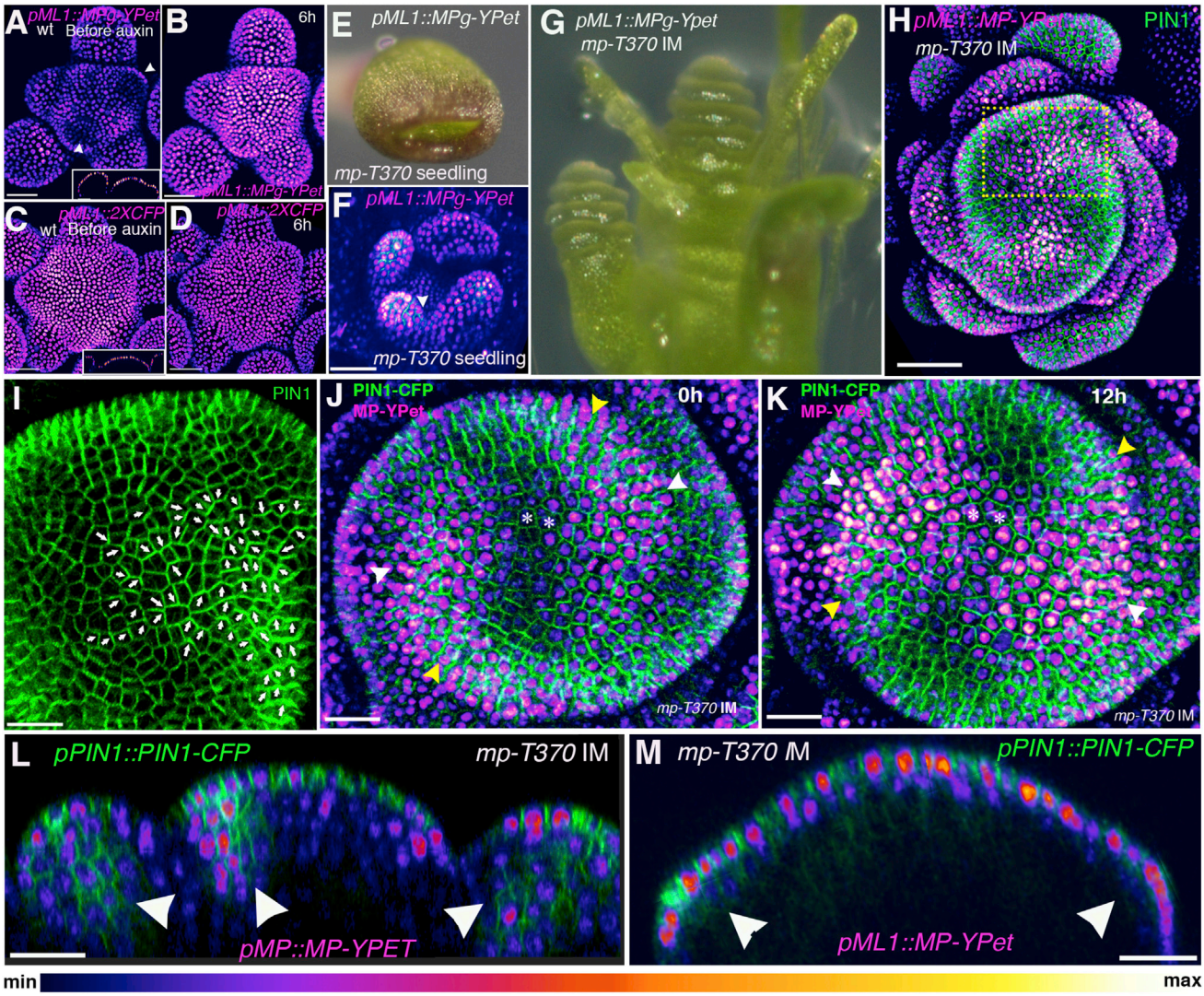

Figure 4. Restriction of MP Activity to the Epidermis Results in Mobile Auxin Maxima

(A and B) *pML1::MP-YPet* expression (magenta) in wild-type before (A) and 6 hr after auxin treatment (B) (n > 20). The inset in (A) shows a longitudinal optical section; white arrowheads in (A) point to regions of low MP-YPet expression, as also seen when MP is driven by its own promoter.

(C and D) *pML1::2X-CFP-N7* expression (magenta) before (C) and 6 hr after auxin treatment (D) (n = 6). The inset in (C) shows a longitudinal optical section showing epidermal localization.

(E) Photograph of the *mp-T370* mutant expressing *pML1::MP-YPet*.

(F) Confocal projection of an *mp-T370* mutant seedling with fused leaves (white arrowhead), with *pML1::MP-YPet* (magenta) and *pPIN1::PIN1-CFP* (green).

(G and H) IM of *mp-T370* expressing *pML1::MP-YPet*; photograph (G) and confocal projection, with *pML1::MP-YPet* (magenta) and *pPIN1::PIN1-CFP* (green) (H).

(I) Magnified view of the dotted rectangle in (H) showing PIN1-CFP forming a convergence pattern. The arrows indicate the estimated PIN1 polarity directions within the cells.

(J and K) Time series of *mp-T370* IMs expressing *pML1::MP-YPet* and *pPIN1::PIN1-CFP* before (J) and 12 hr later (K). Note the change in the position of maximum MP expression (white arrowheads) and PIN1 convergences (yellow arrowheads). The asterisks mark the same cells at 0 hr and at 12 hr time point.

(L and M) Longitudinal reconstructed optical sections of *mp-T370* IM showing *pPIN1::PIN1-CFP* and *pMP::MP-YPet* expression (L) and *pML1::MP-YPet* (magenta) and *pPIN1::PIN1-CFP* (M). Arrowheads indicate PIN1-CFP signal in sub-epidermal layers/pro-vasculature (L) or the absence thereof (M).

Scale bars, 30 μm (A and B), 40 μm (C and D), 50 μm (F and H), and 20 μm (I–M). See also Movie S4.

AUTHOR CONTRIBUTIONS

N.B. carried out all wet lab experiments. N.B. and M.G.H. designed the wet lab experiments, proposed the computer model simulations, and analyzed and interpreted the results. C.O. created most of the transgenic plant lines. B.B. carried out mechanical model simulations and helped design them and analyze their output. A.L. carried out auxin transport simulations and helped design them and analyze their output. H.J. helped design the simulation experiments and analyze their output as well as interpret wet lab experimental results. M.G.H., N.B., and B.B. contributed to writing the manuscript, and H.J. and C.O. helped edit it.

ACKNOWLEDGMENTS

We thank Dr. Atsushi Miyawaki from the RIKEN Brain Science Institute for the VENUS fluorescent protein, which was obtained through an MTA. We thank Prof. Dolf Weijers from Wageningen University for kindly providing seeds for the R2D2 auxin sensor and *mp-B4149* mutant allele. We thank Prof. Ken-ichiro Hayashi, Okayama University of Science, for providing auxinole, and Dr. Adrienne H.K. Roeder for the *pML1::2XCFP-N7*-expressing *Arabidopsis* line. We also thank Monica Pia Caggiano, Pia Sappl, Sevi Durdu, and Kota Miura for technical advice. The research leading to these results received funding from the Australian Research Council (M.G.H.) and European Research Council under the European Union's Seventh Framework Programme (FP/2007-2013)/ERC grant agreement 261081 (M.G.H.). The work was also supported by the European Molecular Biology Laboratory (N.B., C.O., and M.G.H.), EMBL International PhD Programme (N.B.), Gatsby Charitable Foundation (GAT3395/PR4) (H.J.), and Swedish Research Council (VR2013-4632) (H.J.).

Received: June 23, 2016
Revised: August 29, 2016
Accepted: September 22, 2016
Published: November 3, 2016

REFERENCES

1. Jean, R.V., and Barabé, D. (1998). Symmetry in Plants (World Scientific).
2. Okada, K., Ueda, J., Komaki, M.K., Bell, C.J., and Shimura, Y. (1991). Requirement of the auxin polar transport system in early stages of *Arabidopsis* floral bud formation. Plant Cell *3*, 677–684.
3. Reinhardt, D., Mandel, T., and Kuhlemeier, C. (2000). Auxin regulates the initiation and radial position of plant lateral organs. Plant Cell *12*, 507–518.
4. Reinhardt, D., Pesce, E.R., Stieger, P., Mandel, T., Baltensperger, K., Bennett, M., Traas, J., Friml, J., and Kuhlemeier, C. (2003). Regulation of phyllotaxis by polar auxin transport. Nature *426*, 255–260.
5. Benková, E., Michniewicz, M., Sauer, M., Teichmann, T., Seifertová, D., Jürgens, G., and Friml, J. (2003). Local, efflux-dependent auxin gradients as a common module for plant organ formation. Cell *115*, 591–602.
6. Heisler, M.G., Ohno, C., Das, P., Sieber, P., Reddy, G.V., Long, J.A., and Meyerowitz, E.M. (2005). Patterns of auxin transport and gene expression during primordium development revealed by live imaging of the *Arabidopsis* inflorescence meristem. Curr. Biol. *15*, 1899–1911.
7. Jönsson, H., Heisler, M.G., Shapiro, B.E., Meyerowitz, E.M., and Mjolsness, E. (2006). An auxin-driven polarized transport model for phyllotaxis. Proc. Natl. Acad. Sci. USA *103*, 1633–1638.
8. Smith, R.S., Guyomarc'h, S., Mandel, T., Reinhardt, D., Kuhlemeier, C., and Prusinkiewicz, P. (2006). A plausible model of phyllotaxis. Proc. Natl. Acad. Sci. USA *103*, 1301–1306.
9. Stoma, S., Lucas, M., Chopard, J., Schaedel, M., Traas, J., and Godin, C. (2008). Flux-based transport enhancement as a plausible unifying mechanism for auxin transport in meristem development. PLoS Comput. Biol. *4*, e1000207.
10. Heisler, M.G., Hamant, O., Krupinski, P., Uyttewaal, M., Ohno, C., Jönsson, H., Traas, J., and Meyerowitz, E.M. (2010). Alignment between PIN1 polarity and microtubule orientation in the shoot apical meristem reveals a tight coupling between morphogenesis and auxin transport. PLoS Biol. *8*, e1000516.
11. Abley, K., De Reuille, P.B., Strutt, D., Bangham, A., Prusinkiewicz, P., Marée, A.F., Grieneisen, V.A., and Coen, E. (2013). An intracellular partitioning-based framework for tissue cell polarity in plants and animals. Development *140*, 2061–2074.
12. Bayer, E.M., Smith, R.S., Mandel, T., Nakayama, N., Sauer, M., Prusinkiewicz, P., and Kuhlemeier, C. (2009). Integration of transport-based models for phyllotaxis and midvein formation. Genes Dev. *23*, 373–384.
13. Abley, K., Sauret-Güeto, S., Marée, A.F.M., and Coen, E. (2016). Formation of polarity convergences underlying shoot outgrowths. eLife *5*, e18165.
14. Hardtke, C.S., and Berleth, T. (1998). The *Arabidopsis* gene MONOPTEROS encodes a transcription factor mediating embryo axis formation and vascular development. EMBO J. *17*, 1405–1411.
15. Guilfoyle, T.J., and Hagen, G. (2007). Auxin response factors. Curr. Opin. Plant Biol. *10*, 453–460.
16. Liao, C.Y., Smet, W., Brunoud, G., Yoshida, S., Vernoux, T., and Weijers, D. (2015). Reporters for sensitive and quantitative measurement of auxin response. Nat. Methods *12*, 207–210.
17. Lau, S., De Smet, I., Kolb, M., Meinhardt, H., and Jürgens, G. (2011). Auxin triggers a genetic switch. Nat. Cell Biol. *13*, 611–615.
18. Wenzel, C.L., Schuetz, M., Yu, Q., and Mattsson, J. (2007). Dynamics of MONOPTEROS and PIN-FORMED1 expression during leaf vein pattern formation in *Arabidopsis thaliana*. Plant J. *49*, 387–398.
19. Ckurshumova, W., Krogan, N.T., Marcos, D., Caragea, A.E., and Berleth, T. (2012). Irrepressible, truncated auxin response factors: natural roles and applications in dissecting auxin gene regulation pathways. Plant Signal. Behav. *7*, 1027–1030.
20. Fletcher, J.C., Brand, U., Running, M.P., Simon, R., and Meyerowitz, E.M. (1999). Signaling of cell fate decisions by CLAVATA3 in *Arabidopsis* shoot meristems. Science *283*, 1911–1914.
21. Joubès, J., De Schutter, K., Verkest, A., Inzé, D., and De Veylder, L. (2004). Conditional, recombinase-mediated expression of genes in plant cell cultures. Plant J. *37*, 889–896.
22. Dharmasiri, N., Dharmasiri, S., and Estelle, M. (2005). The F-box protein TIR1 is an auxin receptor. Nature *435*, 441–445.
23. Kepinski, S., and Leyser, O. (2005). The *Arabidopsis* F-box protein TIR1 is an auxin receptor. Nature *435*, 446–451.
24. Dharmasiri, N., Dharmasiri, S., Weijers, D., Lechner, E., Yamada, M., Hobbie, L., Ehrismann, J.S., Jürgens, G., and Estelle, M. (2005). Plant development is regulated by a family of auxin receptor F box proteins. Dev. Cell *9*, 109–119.
25. Braybrook, S.A., and Peaucelle, A. (2013). Mechano-chemical aspects of organ formation in *Arabidopsis thaliana*: the relationship between auxin and pectin. PLoS ONE *8*, e57813.
26. Hamant, O., Heisler, M.G., Jönsson, H., Krupinski, P., Uyttewaal, M., Bokov, P., Corson, F., Sahlin, P., Boudaoud, A., Meyerowitz, E.M., et al. (2008). Developmental patterning by mechanical signals in *Arabidopsis*. Science *322*, 1650–1655.
27. Deb, Y., Marti, D., Frenz, M., Kuhlemeier, C., and Reinhardt, D. (2015). Phyllotaxis involves auxin drainage through leaf primordia. Development *142*, 1992–2001.
28. Heisler, M.G., and Jönsson, H. (2006). Modeling auxin transport and plant development. J. Plant Growth Regul. *25*, 302–312.
29. Kierzkowski, D., Lenhard, M., Smith, R., and Kuhlemeier, C. (2013). Interaction between meristem tissue layers controls phyllotaxis. Dev. Cell *26*, 616–628.